

AN INVESTIGATION OF THE STRUCTURE AND DYNAMICS OF AN INTENSE SURFACE FRONTAL ZONE

By *Frederick Sanders*

Massachusetts Institute of Technology¹

(Manuscript received 21 March 1955)

ABSTRACT

Intensive analysis of a pronounced surface frontal zone indicates that the associated horizontal temperature gradient, horizontal wind shear and horizontal divergence are most extreme near the ground and become much more diffuse above the lowest few thousand feet. In an endeavor to account for these structural characteristics, measurements are made of the frontogenetical and frontolytical effects in the fields of temperature and wind, following the motion of the air. In the vicinity of the frontal zone in the lowest levels, these effects are found to be one or two orders of magnitude larger than those generally observed in the free atmosphere. It is indicated that the frontal zone itself is composed of air initially in the warm sector which has been first effectively entrained into the zone through the operation of intense frontogenetical effects and is then subjected to intense frontolysis as it rises within the zone, thus accounting for the observed maximum intensity of the frontal characteristics near the ground. It appears, furthermore, that the motion of this type of frontal zone at the surface is controlled by the motion of the adjacent cold air.

1. Introduction

Marked surface fronts have been recognized as significant features of the atmosphere since J. Bjerknes' (1919) original description of the phenomenon, based upon careful study of data from a dense network of surface reporting stations. Fronts were initially considered as the intersection of the earth's surface

¹The research reported in this article was supported in part by the Office of Naval Research, under Contract No. N5ori-07804.

and a sloping surface of discontinuity with respect to density, existing through a substantial portion of the troposphere; but it was not until some years later that sufficient soundings became available for a study of the three-dimensional aspects of frontal structure. In some of the first of these studies, J. Bjerknes (1932) and J. Bjerknes and Palmén (1937) were able to identify frontal boundaries at the upper levels; but these constituted only first-order discontinuities with respect to density and bounded a frontal zone of con-

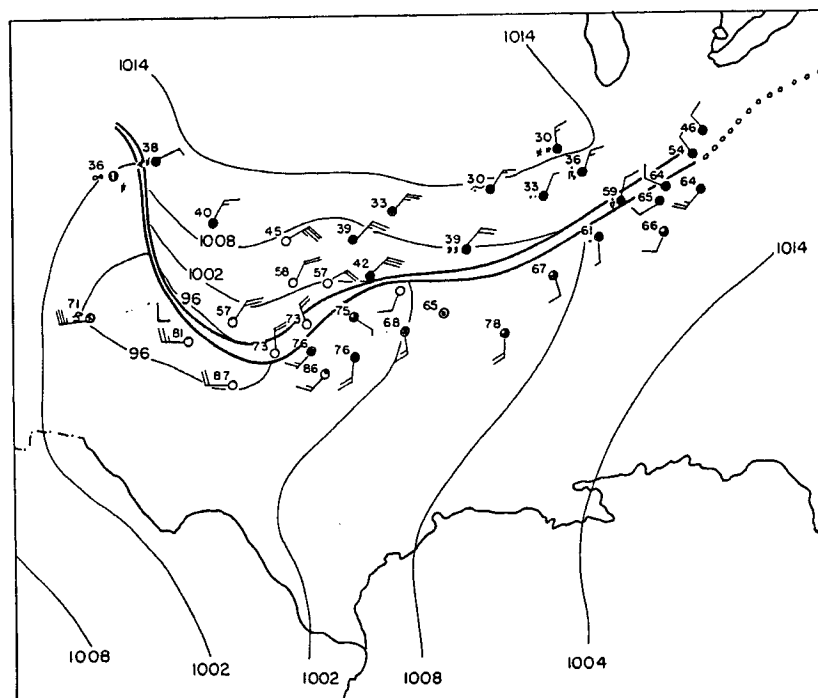


FIG. 1. Surface chart, 2130 GCT 17 April 1953. Heavy solid lines: boundaries of frontal zone. Light solid lines: sea-level isobars at 6-mb intervals. Plotted reports follow conventional station model.

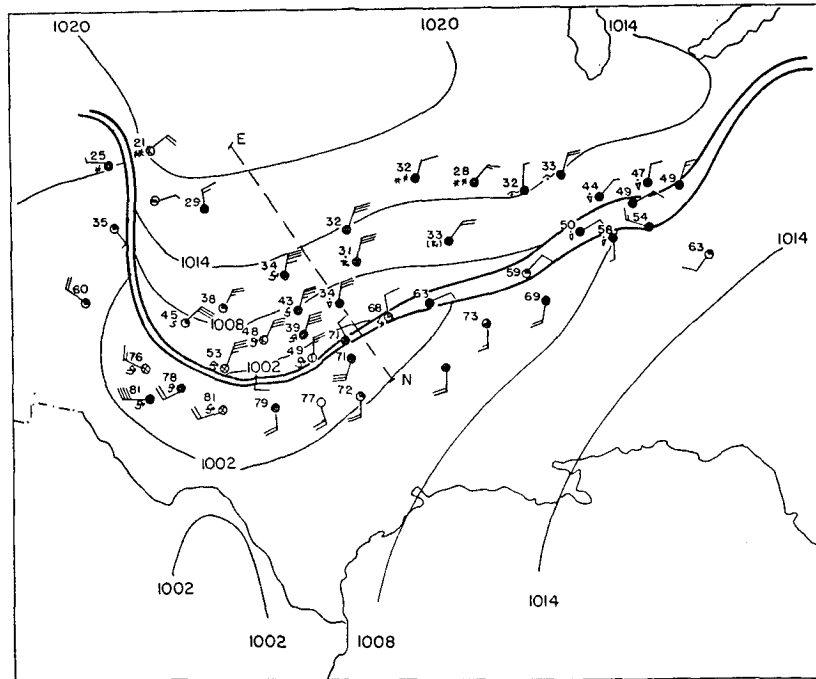


FIG. 2. Same as fig. 1, but for 0330 GCT 18 April 1953. Dashed line E-N indicates position of vertical cross section.

siderable width. More recently, Palmén (1948) has shown the existence of pronounced frontal zones in the middle and upper troposphere. Wide disagreement exists among meteorologists, however, on the question of the vertical extent of surface fronts, and the data have not generally been sufficiently dense to permit a detailed examination of the variation of frontal characteristics with altitude.

Bergeron (1928) studied the kinematical conditions under which the formation of a front might be expected, and a detailed theoretical study of linear fields of horizontal motion by Petterssen (1935) indicated that frontogenesis was favored near the axis of dilatation in a field of deformation. The necessity of considering the development of cyclonic shear in the wind field as part of the frontogenetical process was recognized by

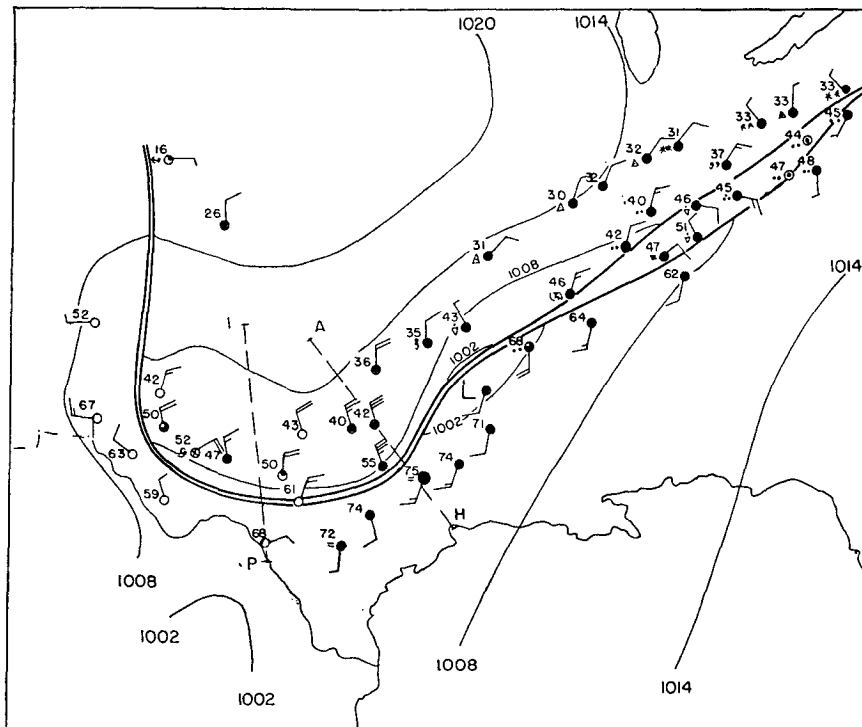


FIG. 3. Same as fig. 1, but for 0930 GCT 18 April 1953. Dashed lines A-H and I-P indicate positions of vertical cross sections.

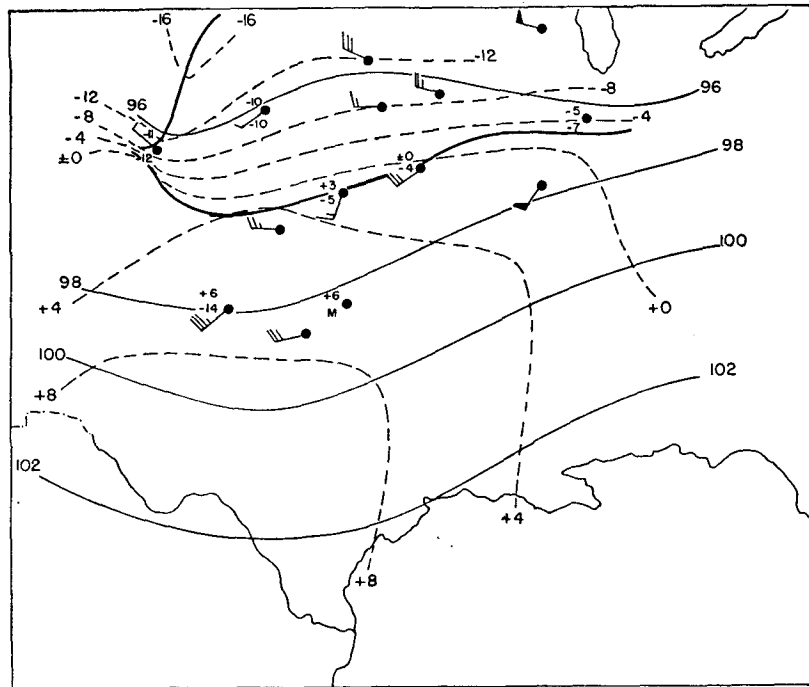


FIG. 4. 700-mb chart, 2100 GCT 17 April 1953. Heavy solid lines: boundaries of the frontal zone. Light solid lines: contours at 200-ft intervals, labelled with tens and units digits omitted. Dashed lines: isotherms at intervals of 4C. Plotted reports follow conventional station model.

Petterssen and Austin (1942). In the latter study, it was suggested that horizontal convergence at the front was responsible for the development of this shear. These investigations, however, considered only the field of horizontal motion, and the data until recently have been insufficient to evaluate the effects upon frontal structure of the field of vertical motion.

An opportunity for a detailed three-dimensional in-

vestigation of frontal structure and behavior arose on 17 and 18 April 1953, when an intense surface front passed southward through the dense network of radio-sonde and upper-level wind stations maintained by the U. S. Weather Bureau and the U. S. Air Force in the south central United States. This case is typical of many marked fronts affecting this area and displays structural characteristics similar to those found by

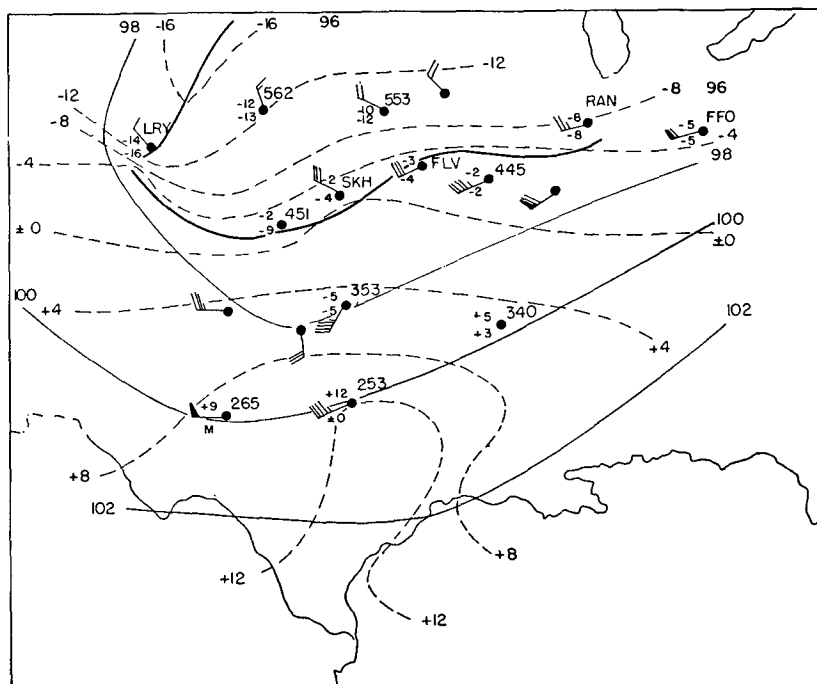


FIG. 5. Same as fig. 4, but for 0300 GCT 18 April 1953. Identification numbers or letters for selected stations are indicated above and to right of station circles.

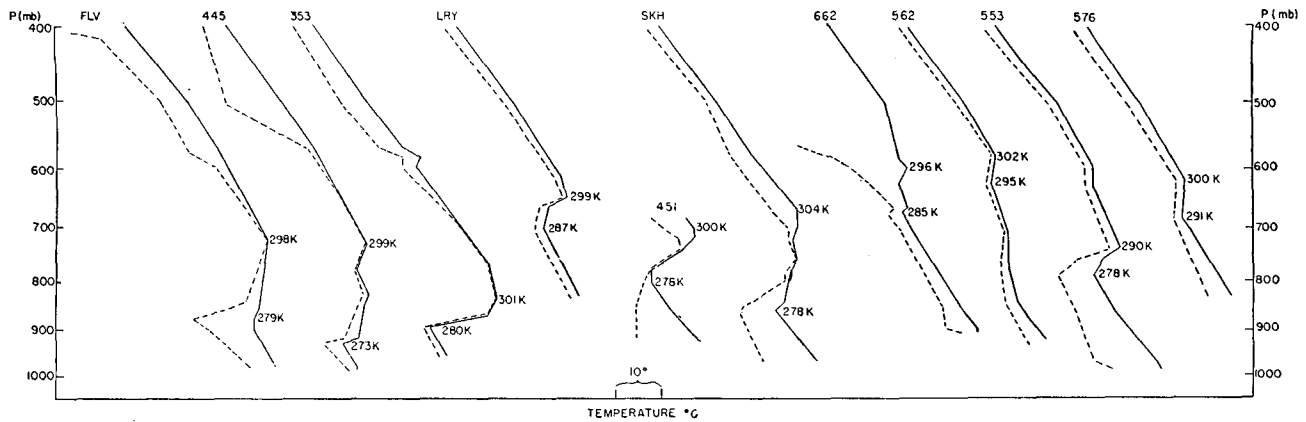


FIG. 8. Soundings illustrating position of frontal zone at 0300 GCT 18 April 1953. Solid lines are temperature soundings. Dashed lines are dew-point soundings.

lower levels increased with time, suggesting that particles initially within the warm air-mass were being incorporated into the frontal zone as it moved southward. In this investigation, detailed measurements of the frontal characteristics in the fields of temperature and motion are made within the frontal zone at various levels. Then the frontogenetical equation of Miller (1948) and an appropriate form of the vorticity equation are applied in an attempt to account for these characteristics, which are believed to be typical of intense surface frontal zones.

2. Structural characteristics of the frontal zone

Information concerning the position and intensity of the frontal zone at the surface was obtained from a study of all pertinent hourly reports in the area under investigation. Isochrones of the zone and the associated 1-hr temperature changes and vector wind-shifts are shown in fig. 7. The entire frontal zone passed a great majority of the stations between successive hourly observations, indicating that the width of the zone was for the most part only a few kilometers at the surface. The position and intensity of the zone in the free atmosphere were determined from a study of all

relevant radiosonde observations, which were available at 6-hr intervals. The frontal soundings at 0300 GCT 18 April are shown in fig. 8, indicating that the discontinuities in lapse rate which determine the upper (warm) and lower (cold) boundaries of the zone are generally clear-cut up to about 700 mb. After location of the frontal zone on the various upper-level charts, analyses of the fields of temperature and observed horizontal wind were made.

The detailed measurements in this study were made with reference to three cross-sections along lines indicated in figs. 2 and 3. The position of the frontal zone and the fields of temperature and wind on these sections were rendered consistent with all other analyses. Horizontal divergence was measured from analyses of the observed winds at 1000-ft intervals up to 6000 ft. These measurements were performed over adjoining rectilinear areas of about 10^4 km², by the "streamline" technique described by Panofsky (1951). Vertical velocities were computed from the horizontal divergence distribution, through the equation of continuity. Measurement of gradients and multiplications and additions required in the frontogenetical equations were accomplished graphically, by the procedure out-

TABLE 1. Frontal characteristics for selected vertical cross-sections, 17 and 18 April 1953.

Section	Alt. (ft) above ground	Width (km) of frontal zone	Horiz. pot. temp. grad. (deg C/10 ³ cm) within zone	Horiz. shear (10 ⁻⁴ sec ⁻¹) within zone*	Horiz. div. (10 ⁻⁶ sec ⁻¹) within zone	Change in parallel comp. of actual wind (m/sec) upward through zone	Change in parallel comp. of geos. wind (m/sec) upward through zone
E-N	1000	25	56	+8.8	-44	17	95
	2000	45	38	+5.6	-35	23	79
	3000	130	15	+2.2	-5	23	39
	4000	215	10	+1.3	-7	34	38
I-P	1000	45	33	+1.6	-25	9	32
	2000	160	11	+0.8	-8	11	22
	3000	270	8	+1.0	-1	17	26
A-H	1000	25	48	+2.8	-23	9	87
	2000	160	12	+0.8	-8	11	24
	3000	330	7	+0.5	-4	19	20

* Positive values indicate cyclonic shear.

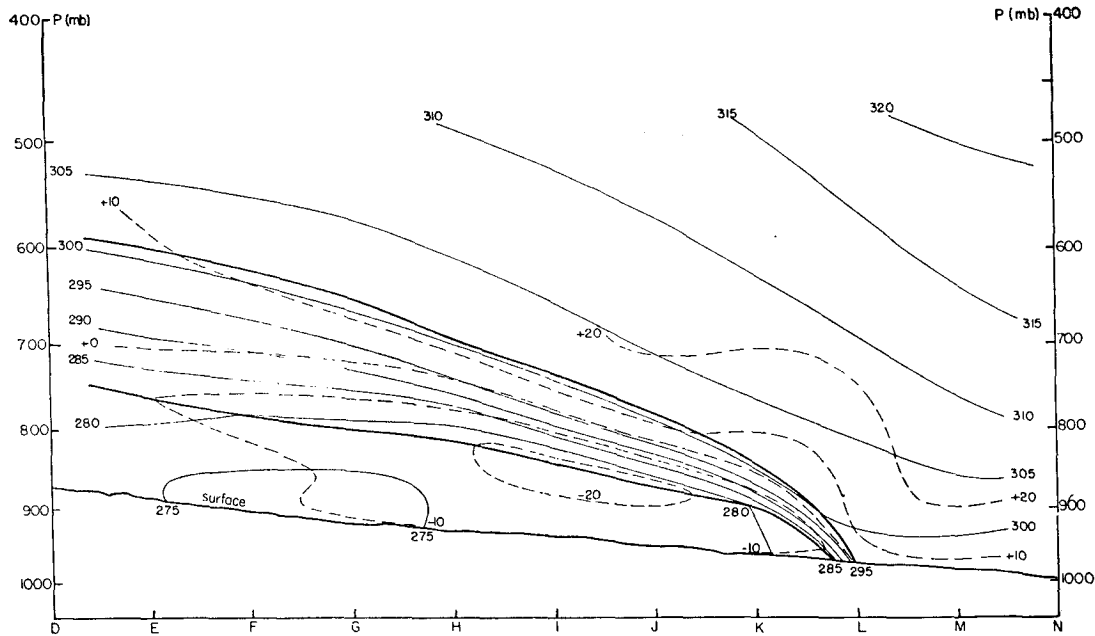


FIG. 9. Distributions of potential temperature and horizontal wind component normal to cross-section E-N, 0300 GCT 18 April 1953. Heavy solid lines: boundaries of frontal zone. Light solid lines: potential isotherms at intervals of 5 K. Dashed lines: isopleths of wind component normal to cross section at intervals of 10 m/sec, positive value representing flow directed into plane of section.

lined by V. Bjerknes (1911). While it might seem that the limits of accuracy of the data and analyses are being strained, it will be seen that the magnitudes of the important derived quantities are so large that relatively large uncertainties in their determination will not obscure the final results.

Measurements of several frontal characteristics observed in cross-sections along the lines E-N, A-H and I-P, shown in figs. 2 and 3, are summarized in table 1. The observed distribution of potential temperature, horizontal divergence, and components of motion in the vertical and in a direction normal to the frontal zone are shown, for the first section, in figs. 9 and 10. From this information it is evident that the width of the frontal zone is smallest and the frontal gradients of temperature and wind are most intense at the lowest levels, where the values of the gradients are

between one and two order of magnitude larger than those generally observed in the free atmosphere. Examination of hourly surface reports indicates that these frontal characteristics are even more marked at the ground itself. At only a few thousand feet above the ground, the zone is much broader and the gradients of temperature and wind are much less extreme. The frontal zone at the ground closely approximates a strong line of convergence, in agreement with J. Bjerknes' (1919) initial description of the phenomenon and with Petterssen and Austin's (1942) findings. The general rising motion of the warm air relative to the cold air is also compatible with the classical frontal concept. The "jet" of extremely intense rising motion immediately above the position of the zone at the ground has important ramifications in the calculation of frontogenetical effects discussed below.

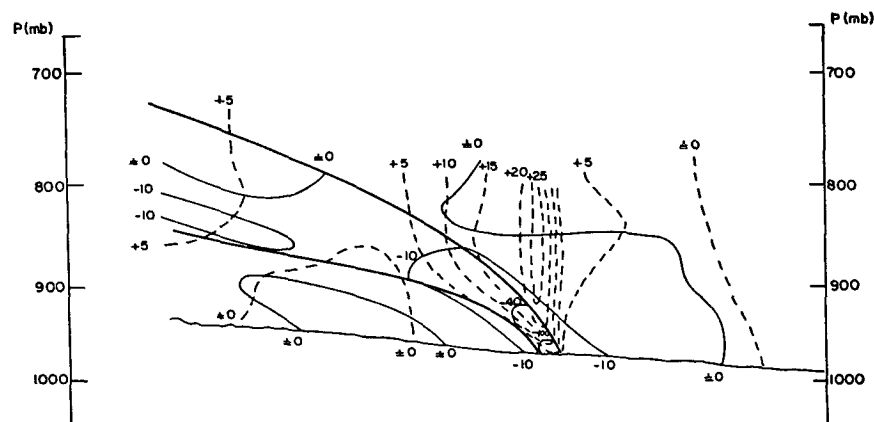


FIG. 10. Distributions of horizontal divergence and vertical motion for part of cross section E-N. Heavy solid lines: boundaries of frontal zone. Light solid lines: selected isopleths of divergence, labelled in units of 10^{-5} sec^{-1} . Dashed lines: isopleths of vertical velocity at intervals of 5 cm/sec.

3. Frontogenetical processes in the fields of potential temperature and wind

It is possible to account for the significant features of the frontal zone in the field of potential temperature by a study of the distribution of frontogenetical and frontolytical effects following the motion of the air. An appropriate expression, derived from the work of Miller (1948) and utilized by Reed and Sanders (1953) in an investigation of frontogenesis at the higher levels, is

$$-\frac{d}{dt} \left(\frac{\partial \theta}{\partial y} \right) = -\frac{\partial}{\partial y} \left(\frac{d\theta}{dt} \right) + \frac{\partial v}{\partial y} \frac{\partial \theta}{\partial y} + \frac{\partial w}{\partial y} \frac{\partial \theta}{\partial z}, \quad (1)$$

where d/dt indicates differentiation following the three-dimensional motion, the y -axis is oriented parallel to the horizontal temperature gradient and directed toward the colder air, and variations in the x -direction are neglected. The first term on the right-hand side of (1), representing the effect of non-adiabatic heating and cooling, is not considered quantitatively in the present investigation. Some qualitative remarks concerning the probable effects of this term are included in the closing discussion.

The instantaneous pattern of frontogenetical and frontolytical effects arising from the second term (confluence term) on the right-hand side of (1) was calculated from the gradients of temperature and motion in cross section E-N and is shown in fig. 11. The results are expressed as 3-hr changes of temperature gradient in degrees Celsius per 100 km. It is seen that the effect is strongly frontogenetical within the frontal zone, particularly near the ground, owing to the coincidence of large values of confluence and temperature gradient. Outside the frontal zone, the effect is relatively small. Similarly, the pattern of frontogenetical and frontolytical effects arising from the third term (tilting term) on the right-hand side of (1) for the cross section E-N is shown in fig. 12. Intense frontogenesis is indicated in the warm air immediately adjacent to the position of the frontal zone at the ground, owing to the intense positive gradient of vertical motion. Within the zone, the effect is generally frontolytical, extremely so in the lower levels due to a coincidence of large negative gradient of vertical motion and large stability. Elsewhere the effect is relatively small.

The net effect of the confluence and tilting mechanisms is shown in fig. 13. The intense frontogenesis arising from the latter mechanism appears virtually unchanged in the warm air adjacent to the position of the frontal zone at the ground. Within the zone, the two mechanisms tend to be in opposition. The frontogenetical influence of the confluence is strongly predominant only in the lowest 1000 ft or so, while the tilting term is responsible for the strong net frontolysis indicated from about 1000 to 4000 ft above the ground.

Even the net value of the effects at several points is probably two orders of magnitude larger than that observed in the absence of frontal zones.

It was suggested above that the warm air-mass near the ground appears to move relative to the frontal zone from right to left across a section such as E-N, later appearing within the frontal zone at some distance above the ground. A typical path might be along the path ABCD in fig. 13. With reference to this figure and with the assumption that the pattern constitutes

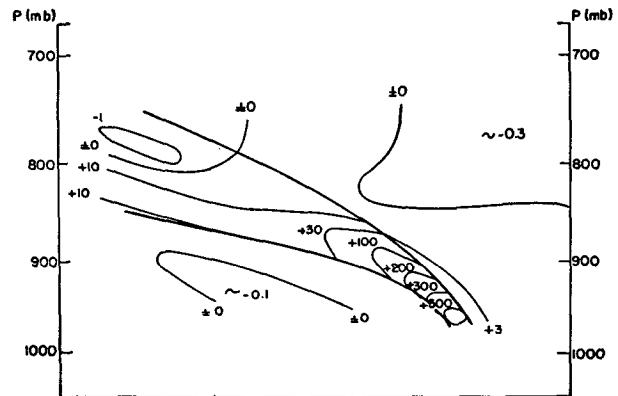


FIG. 11. Frontogenetical effect $(\partial v/\partial y)(\partial \theta/\partial y)$ for part of cross section E-N. Units expressed as 3-hr changes in horizontal temperature gradient in $(\text{deg C})(100 \text{ km})^{-1}$. Positive values indicate frontogenesis in temperature field.

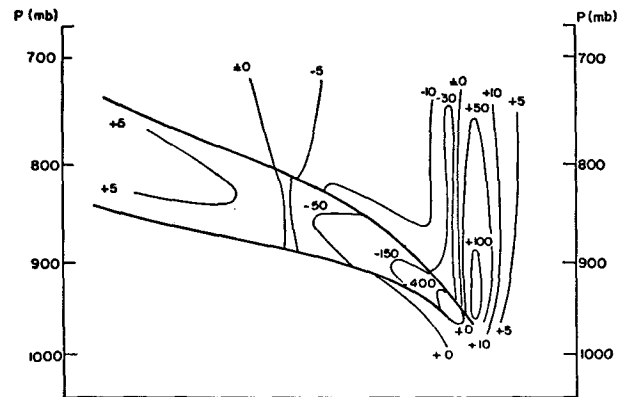


FIG. 12. Frontogenetical effect $(\partial w/\partial y)(\partial \theta/\partial z)$ for part of cross section E-N. Units as in fig. 11.

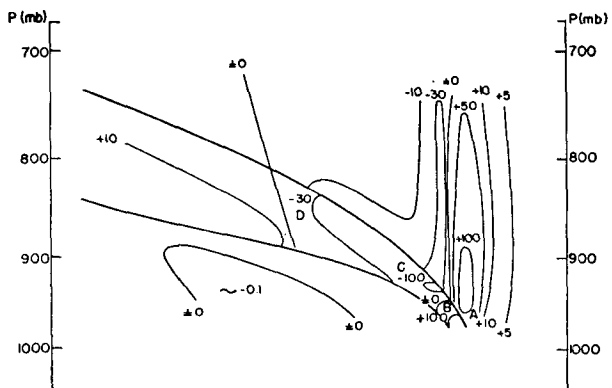


FIG. 13. Net frontogenetical effect, $(\partial w/\partial y)(\partial \theta/\partial z) + (\partial v/\partial y)(\partial \theta/\partial y)$, for part of cross section E-N. Units as in fig. 12.

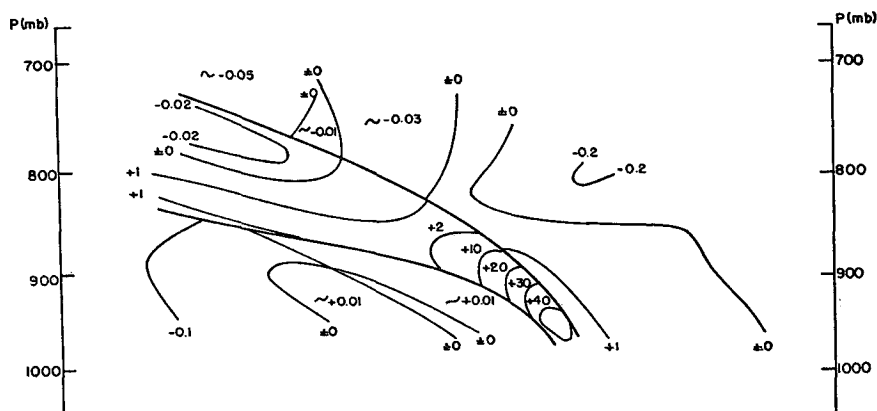


FIG. 14. Frontogenetical effect $(\partial v/\partial y)(\partial u/\partial y)$ for part of cross section E-N. Units expressed as 3-hr changes in horizontal wind shear, in units of 10^{-4} sec^{-1} . Positive values indicate frontogenesis in field of motion.

approximately a steady state, it may be seen that at point A the air is exposed to intense frontogenesis until it acquires a temperature gradient characteristic of the frontal zone. This process is tantamount to entrainment into the frontal zone, and thus the warm boundary of the zone between A and B cannot be considered a substantial surface. At point B, the air perhaps has undergone some further frontogenesis due to the predominant confluence effect within the zone. At point C, however, the air is exposed to intense frontolysis owing to the predominance of the tilting mechanism in this region. The air then arrives at point D with a temperature gradient much less pronounced than that which characterized it at point B. This sequence of events offers an explanation of both the maximum intensity of the frontal temperature gradient near the ground and the apparent entrainment of warm air into the frontal zone.

It is possible to investigate the development and dissipation of the strong cyclonic shear, characteristic of the frontal zone, with the aid of an appropriate form of the vorticity equation for frictionless flow. Such an expression is

$$-\frac{d}{dt} \left(\frac{\partial u}{\partial y} \right) = \frac{\partial v}{\partial y} \frac{\partial u}{\partial y} + \frac{\partial w}{\partial y} \frac{\partial u}{\partial z} - f \frac{\partial v}{\partial y} - \frac{df}{dt}, \quad (2)$$

where, as above, d/dt refers to differentiation following the three-dimensional motion of the air, the y -axis is oriented parallel to the temperature gradient and directed toward the colder air, and all variations in the x -direction have been neglected. The first two terms on the right-hand side of (2) are analogous to terms on the right-hand side of (1). Thus, the first term represents the effect of confluence in changing the magnitude of the horizontal shear. The second term refers to the effect of a horizontal gradient of vertical motion in changing the inclination of surfaces of equal value of the u -component of the wind, thereby altering the horizontal shear. The third term on the right-hand side of (2) represents the production of horizontal shear due to the effects of Coriolis force and has no analogue in the frontogenetical equation for the temperature field. The last term can be shown to be substantially smaller than the others and was neglected.

The effect of the confluence term in (2) was determined for the cross section E-N through measurement of the gradients of the horizontal and vertical components of motion. The resultant pattern is shown in fig. 14, in which the effects are represented as 3-hr changes of shear in units of 10^{-4} per second, the approximate value of the Coriolis parameter in middle

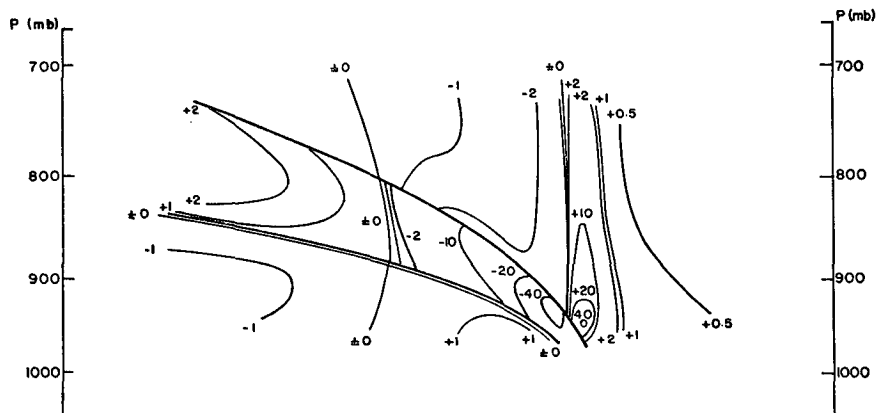


FIG. 15. Frontogenetical effect $(\partial w/\partial y)(\partial u/\partial z)$ for part of cross section E-N. Units as in fig. 14.

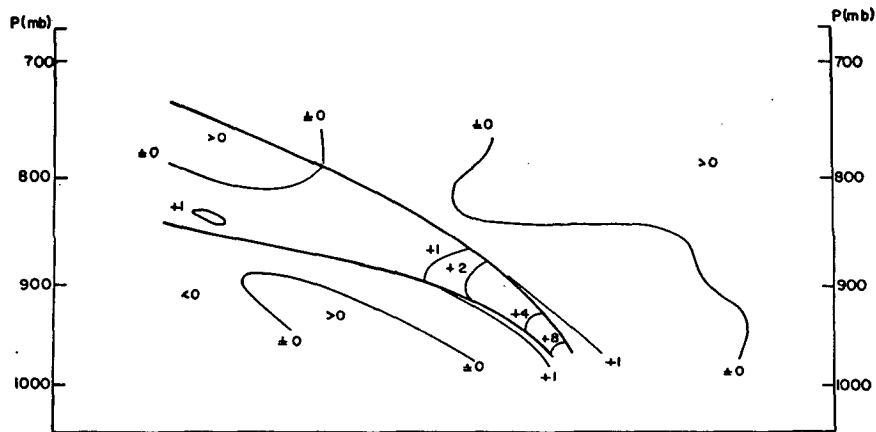


FIG. 16. Frontogenetical effect $-f \partial v / \partial y$ for part of cross section E-N. Units as in fig. 14.

latitudes. It is seen that the pattern is similar to that shown in fig. 11 for the temperature field. That is, the effect is strongly frontogenetical within the lower portion of the frontal zone, owing to a coincidence of strong confluence and strong horizontal shear. Outside the zone, this effect is relatively small. Similarly, the effect of the tilting mechanism in altering the horizontal shear is depicted for the section E-N in fig. 15. The effect is strongly frontogenetical in the warm air adjacent to the position of the frontal zone at the ground, due to the intense horizontal gradient of vertical motion. Within the lower portion of the zone, the effect is strongly frontolytical due to the negative gradient of vertical motion and the strong vertical wind shear. Elsewhere the effect is relatively small. The effect of the third term on the right-hand side of (2) is shown in fig. 16. Though smaller than either the confluence or tilting effect, this term yields appreciable frontogenetical effects in the lowest portion of the frontal zone.

The sum of the three above effects is shown in fig. 17. On the assumption, as in the discussion of the temperature field, that this distribution represents approximately a steady state, the motion of air along a path such as ABCD in fig. 17 is considered. The sequence of events is quite similar to that described in

the case of the temperature field. At point A, the air is subject to intense frontogenesis with respect to the wind field and is effectively entrained into the frontal zone. At point B, the air attains its maximum horizontal shear owing to further frontogenesis within the frontal zone. At point C, rapid frontolysis is occurring; so the air arrives at point D with substantially smaller shear than it possessed at lower levels, though the diminution is not as pronounced as in the case of the temperature field. The region of frontogenesis indicated in fig. 17 near the lower boundary of the frontal zone, between 850 and 800 mb, is not consistent with the observed weakness of the frontal zone at the 700-mb level and may be non-representative or spurious. In any case, as regards the cyclonic shear characterizing the frontal zone, this account offers an explanation of the maximum intensity of the zone near the ground and of the entrainment of warm air into the frontal zone. As in the case of the temperature field, the frontogenetical and frontolytical processes are phenomenally intense compared with what is generally observed in the free atmosphere. It is perhaps noteworthy that this is so even with a frontal zone which appears to have approximately uniform intensity as an entity on the weather map.

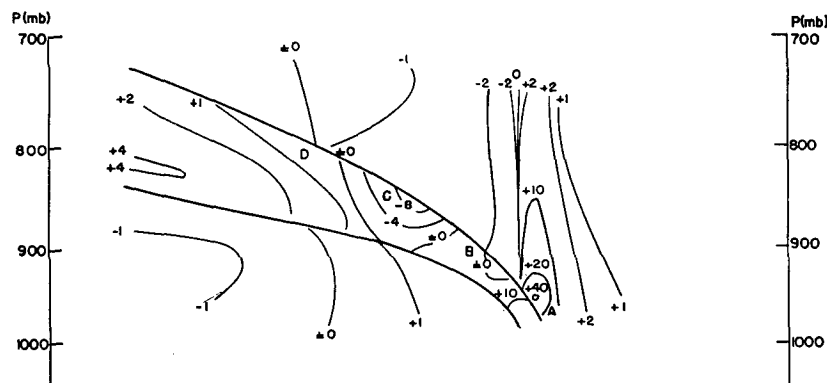


FIG. 17. Net frontogenetical effect, $(\partial w / \partial y)(\partial u / \partial z) + (\partial v / \partial y)(\partial u / \partial y) - f \partial v / \partial y$ for part of cross section E-N. Units as in fig. 14.

The foregoing discussion contains implications concerning the motion of the frontal zone. The evidence of entrainment of warm air into the zone near the ground indicates that the warm boundary of the zone in this region is not a substantial boundary. No such entrainment, however, is indicated at the cold boundary of the zone. Hence, it might be expected that the motion of the zone near the ground is determined by the horizontal motion of the adjacent cold air. As a test of this hypothesis, the component of surface wind normal to the frontal zone was computed from the report from each station in the area under investigation at the hour subsequent to frontal passage. This component is compared in fig. 18 to the speed of the frontal zone as it passed each station. It appears that a line of best fit to the data would approximately equate the speeds of the zone and of the normal component of motion in the cold air at the surface. The correlation is not particularly high; but the result is felt to be satisfactory, in view of the difficulty of obtaining representative measurements of the two quantities involved.

Another aspect which may be touched upon briefly is the development of the vertical shear of the wind component parallel to the frontal zone. It is possible to study the changes in this shear, again following the motion of the air, with a form of the equation describing changes in vorticity about the y -axis. It is

$$\frac{d}{dt} \left(\frac{\partial u}{\partial z} \right) = - \frac{\partial w}{\partial z} \frac{\partial u}{\partial z} - \frac{\partial v}{\partial z} \frac{\partial u}{\partial y} + f \frac{\partial v}{\partial z}, \quad (3)$$

in which inviscid flow is assumed, the y -axis is directed

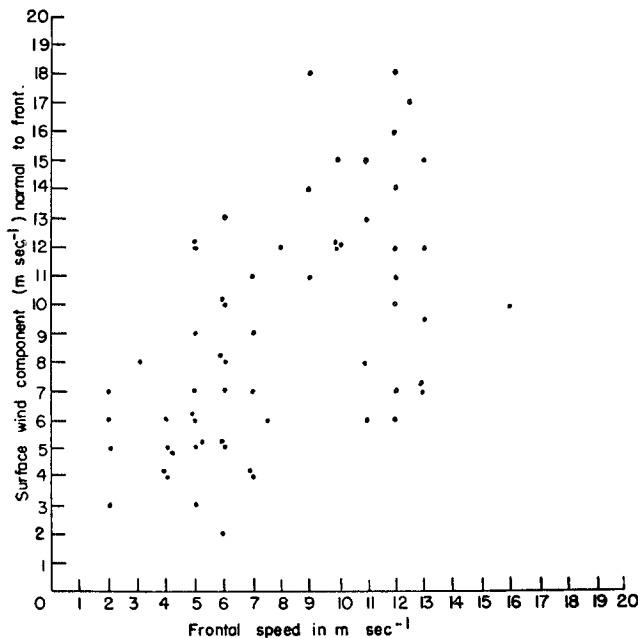


FIG. 18. Relationship between speed of frontal zone of 17 and 18 April 1953 at surface and surface wind component normal to frontal zone in adjacent cold air.

as before, and variations in the x -direction are neglected.

The terms on the right-hand side of (3) are quite analogous to corresponding terms in (2). Thus, the first term may be considered a "vertical confluence" term, the second a tilting effect produced by vertical variation in the v -component of the wind, and the third a Coriolis term expressing the effects of the rotation of the earth. The terms may all be of the same order of magnitude. With reference to the cross section E-N in figs. 9 and 10, it may be seen that the vertical and horizontal variations of u and the vertical variation of w are small outside the frontal zone. The vertical variation of v , which is essentially equivalent to the divergence in the present case, is large only within the lower portion of the zone. It is evident, therefore, that none of the terms in (3) acts strongly outside the frontal zone. Within the zone, however, the vertical-confluence term acts to destroy the vertical shear, owing to the upward increase in the vertical component of motion. The tilting and Coriolis terms, on the other hand, tend to increase the vertical shear and are evidently predominant. The entrainment process involves rapid development of horizontal shear, as discussed above, but leaves the vertical shear practically unchanged. Once the air has entered the frontal zone, however, its vertical shear increases until it rises to the level at which the divergence (i.e., $\partial v/\partial z$) becomes relatively small. At this level, it is likely that the flow is much more nearly geostrophic than at lower levels. This view is confirmed very satisfactorily by the data in the two right-hand columns of table 1. It may be seen that the vertical shear within the frontal zone increases with altitude, while the corresponding geostrophic vertical shear (calculated with the aid of the thermal wind equation) decreases. At 3000 or 4000 ft above the ground, where the values of actual and geostrophic vertical shear are nearly in agreement, the former appears to reach its maximum.

Less detailed measurements of frontogenetical processes in the fields of temperature and wind have been made for a number of additional frontal cross-sections, and the patterns of all these effects resemble those described above. It appears, in fact, that any surface frontal zone, characterized by a structure similar in the fields of temperature and wind to that shown in the cross section E-N and by an intense maximum of convergence near the ground, would display a similar pattern of frontogenetical and frontolytical effects, since the pattern of vertical motion would resemble that shown in fig. 10.

The structure of this type of frontal zone at the surface itself can only be understood through a study of small-scale eddy effects. The above analysis indicates intense net frontogenesis in this region, due to confluence. Presumably the eddy effects are frontolytical,

but it is not possible to investigate the matter quantitatively at the present time. In the present investigation, furthermore, dry-adiabatic processes were assumed, and the most significant patterns of frontogenesis and frontolysis were in fact found below the level at which condensation was occurring. Release of latent heat should be taken into account, however, for a fuller understanding of this type of frontal zone above the condensation level.

With reference to the general effects of non-adiabatic heating and cooling in this case, the configuration of the potential isotherms near the ground in fig. 9 indicates that lapse rates in the cold air are close to the dry-adiabatic rate, while those within the warm air are smaller than the dry-adiabatic lapse rate. Thus, it is indicated that the cold air is perhaps being heated by the earth's surface; and it is indeed observed that the temperature at the cold boundary of the frontal zone near the ground increases at the rate of a few degrees Celsius per day. In the lowest portions of the warm air adjacent to the frontal zone, however, the vertical gradient of potential temperature suggests slight non-adiabatic cooling. It is unlikely, therefore, that the observed warming with time along the warm boundary might arise from non-adiabatic heating. Within the frontal zone, the effects of small-scale turbulence would almost certainly be to decrease the horizontal and vertical gradients of potential temperature, *i.e.*, to produce a heating at the cold boundary and a cooling at the warm boundary.

From the above discussion, it is evident that the net frontogenetical mechanism for this type of frontal zone is concentrated in the lowest levels. It follows, then, that the appearance of this type of zone aloft is a result of vertical transport of air which has acquired frontal characteristics near the ground. Thus, in the area of general rising motion and strong winds aloft ahead of a cyclone, the zone may appear at higher levels over a considerable area in advance of the surface center, though in a much weaker state than near the ground. Along the portion of the cold front to the rear of the cyclone, the lifting of air within the frontal zone is probably weaker, and the air aloft is probably advancing approximately as rapidly as the cold front at the surface. This portion of the frontal zone, therefore, may have little extent in space.

It should be pointed out that the mechanism responsible for the production of this type of frontal zone is entirely different from that described by Reed and Sanders (1953), Newton (1954), and Reed (1955) with reference to an intense type of frontal zone in the middle and upper troposphere. There appears to be no reason why the two types of zone should adjoin directly in space, even when they are simultaneously present in the same general region. The independence

of the two types of zone has been noted by Newton (1954).

4. Conclusions

In summary, the principal conclusions of this study are listed below:

1. The intense surface frontal zone attains maximum strength near the ground and weakens rapidly with altitude.
2. Warm air is entrained into this type of frontal zone near the ground.
3. These aspects in the fields of both temperature and wind can be explained by a consideration of the pattern of frontogenetical and frontolytical effects following the motion of the air.
4. These frontogenetical and frontolytical effects are extremely intense in the vicinity of marked frontal zones, attaining values one or two orders of magnitude larger than those generally observed in the free atmosphere.
5. The intense surface frontal zone tends to move with the adjacent cold air at or very near the ground.

Acknowledgments.—The writer wishes to express his gratitude to Profs. J. M. Austin of the Massachusetts Institute of Technology, and R. J. Reed of the University of Washington, for their helpful suggestions and comments during the course of this work, and to Miss I. Kole for the drafting of the diagrams.

REFERENCES

- Bergeron, T., 1928: Über die dreidimensional verknüpfende Wetteranalyse. *Geofys. Publ.*, 5, No. 6, 73–78.
- Bjerknes, J., 1919: On the structure of moving cyclones. *Geofys. Publ.*, 1, No. 2.
- , 1932: Explorations de quelques perturbations atmosphériques à l'aide de sondages rapprochés dans le temps. *Geofys. Publ.*, 9, No. 9.
- , and E. Palmén, 1937: Investigations of selected European cyclones by means of serial ascents. *Geofys. Publ.*, 12, No. 2.
- Bjerknes, V., and collaborators, 1911: *Dynamic meteorology and hydrology*. (Part II, Kinematics), Washington, Carnegie Inst.
- Miller, J. E., 1948: On the concept of frontogenesis. *J. Meteor.*, 5, 169–171.
- Newton, C. W., 1954: Frontogenesis and frontolysis as a three-dimensional process. *J. Meteor.*, 11, 449–461.
- Palmén, E., 1948: On the distribution of temperature and wind in the upper westerlies. *J. Meteor.*, 5, 20–27.
- Panofsky, H. A., 1951: Large-scale vertical velocity and divergence. *Compendium Meteor.*, Boston, Amer. meteor. Soc., 639–646.
- Petterssen, S., 1935: Contribution to the theory of frontogenesis. *Geofys. Publ.*, 11, No. 6.
- , and J. M. Austin, 1942: Fronts and frontogenesis in relation to vorticity. *Pap. phys. Ocean. Meteor., Mass. Inst. Tech. and Woods Hole ocean. Instn.*, 7, No. 2, 37 pp.
- Reed, R. J., 1955: A study of a characteristic type of upper-level frontogenesis. *J. Meteor.*, 12, 226–237.
- , and F. Sanders, 1953: An investigation of the development of a mid-tropospheric frontal zone and its associated vorticity field. *J. Meteor.*, 10, 338–349.
- Sanders, F., 1954: *An investigation of atmospheric frontal zones*. (Unpubl. Sc.D. Dissert.), Cambridge, Mass. Inst. Tech.